Seismic Testing of Repaired Unreinforced Masonry Building having Flexible Diaphragm

Jocelyn Paquette[1]; Michel Bruneau, M.ASCE[2]; and Svetlana Brzev[3]

Abstract: The in-plane rocking behavior of unreinforced masonry walls is generally perceived as a stable desirable behavior. However, there may be instances where the available lateral resistance of such walls would be inadequate. In that perspective, fiberglass strips were applied to damaged unreinforced masonry (URM) shear walls to increase their in-plane lateral load-resisting capacity. This paper reports on the dynamic response and behavior of a full-scale one-story unreinforced brick masonry building specimen having a flexible wood floor diaphragm. The shear walls were damaged in a previous test and repaired with fiberglass strips. The results demonstrate the effectiveness of fiberglass strips in enhancing the in-plane seismic response of URM walls failing in rocking and bed joint sliding mode. The response of the wood diaphragm and its interaction with the shear walls have also been studied. As a consequence of the increased in-plane lateral resistance of URM shear wall, the diaphragm was subjected to larger deformations in the inelastic range. The evaluation of experimental results and the comparison with the existing procedures have revealed that the diaphragm deflections observed experimentally closely matched those predicted using the Federal Emergency Management Agency 356 and Agbabian, Barnes, and Kariotis models.

DOI: 10.1061/(ASCE)0733-9445(2004)130:10(1487)

CE Database subject headings: Masonry; Seismic response; Fiber reinforced materials; Earthquakes; Tests; Wood floors; Diaphragms; Rehabilitation.

Introduction

The seismic hazard posed by old unreinforced masonry building (URM) has been long recognized. The deficient seismic strength and/or ductility of many older existing URM buildings is a problem in most of North America, and many URM buildings would suffer damage or even collapse in the event of a severe earthquake. However, as reported during major earthquakes, URM buildings can perform surprisingly well under certain circumstances. Numerous tests have been conducted to study and analyze the seismic behavior of unreinforced masonry buildings. It has been shown in the literature that, for shear walls and piers subjected to in-plane loading, after initial flexural cracking, a stable rigid-body rocking motion could develop, exhibiting moderate ductility (ABK 1984; Epperson and Abrams 1990; Prawel and Lee 1990; Bruneau 1994; Costley and Abrams 1995). This rigid-body mechanism is recognized by the Uniform Code for Building Conservation (UCBC) (ICBO 1997) to be a favorable stable failure mechanism.

The in-plane rocking behavior of unreinforced masonry walls is classified by Federal Emergency Management Agency (FEMA) 273 (FEMA 1997) as a "displacement-controlled" action. This behavior is characterized with rather large postcracking deformations that remain stable for many cycles (FEMA 1999a). However, there may be instances where the available lateral resistance of such walls would be inadequate. In that perspective, a possible retrofit strategy might consist of strengthening the shear walls and piers with vertical fiberglass strips installed to preserve the desirable in-plane pier rocking mode while increasing the lateral strength and ductility. An additional benefit of the fiberglass strips installed in this manner would be the enhanced out-of-plane wall resistance (which is beyond the scope of this study).

Pseudodynamic tests on a full-scale one-story unreinforced brick masonry specimen having a flexible wood floor diaphragm were conducted to investigate the effectiveness of the proposed strategy. Following the initial series of tests performed to assess the behavior of the existing structure (Paquette and Bruneau 2003), the damaged shear walls were repaired using fiberglass strips. Given that constructing another specimen was not possible within the available research budget, behavior of this repaired specimen is taken here as a proxy of the behavior of a retrofitted structure. Results presented are also representative of how a building repaired per the procedure presented here would perform in a subsequent earthquake. In this paper, the dynamic response of the repaired shear walls is analyzed, as well as the response of the wood diaphragm and its interaction with the shear walls.

[1]Conservation Engineer, Heritage Conservation Program, Public Works and Government Services Canada, 25 Eddy, Gatineau, Quebec, Canada K1A 0M5. E-mail: Jocelyn.Paquette@pwgsc.gc.ca

[2]Professor and Director, Dept. of Civil and Environmental Engineering, Multi-Disciplinary Centre for Earthquake Engineering Research, 130 Ketter Hall, State Univ. of New York, Buffalo, NY 14260. E-mail: bruneau@acsu.buffalo.edu

[3]Instructor, British Columbia Institute of Technology, 3700 Willingdon Ave., Burnaby, British Columbia, Canada V5G 3H2. E-mail: sbrzev@bcit.ca

Note. Associate Editor: Sanj Malushte. Discussion open until March 1, 2005. Separate discussions must be submitted for individual papers. To extend the closing date by one month, a written request must be filed with the ASCE Managing Editor. The manuscript for this paper was submitted for review and possible publication on December 11, 2002; approved on February 5, 2004. This paper is part of the ***Journal of Structural Engineering***, Vol. 130, No. 10, October 1, 2004. ©ASCE, ISSN 0733-9445/2004/10-1487–1496/$18.00.

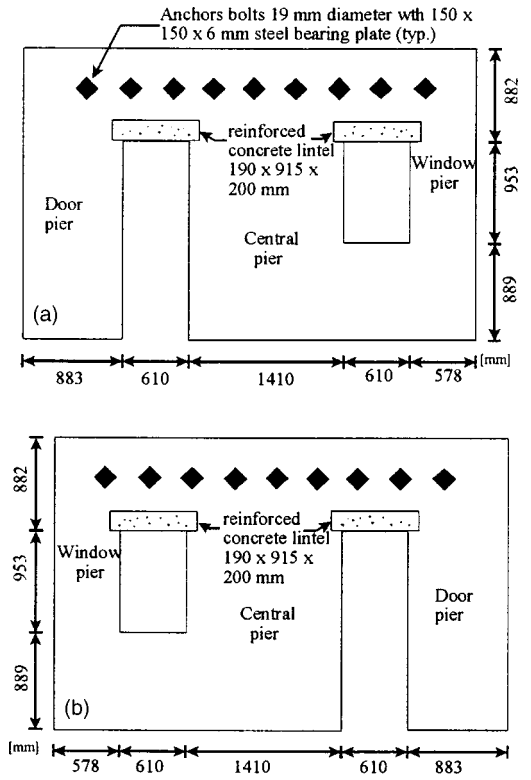

Fig. 1. Elevation of unreinforced masonry specimen (parallel to loading): (a) east wall and (b) west wall

Original Unreinforced Masonry Specimen

Description of Specimen

The single-story full-scale unreinforced brick masonry building used in the experimental study is shown in Figs. 1–3. The building plan dimensions were approximately 4 m width $\times$ 5.6 m length, whereas the wall height and thickness were 2.7 m and 190 mm, respectively. Shear walls were designed such that all piers would successively develop a pier-rocking behavior during seismic response. Among noteworthy features of this specimen,

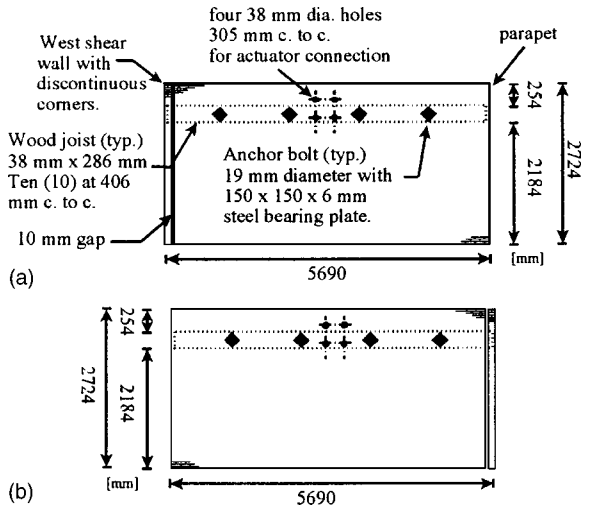

Fig. 2. Elevation of unreinforced masonry specimen (normal to loading): (a) south wall and (b) north wall

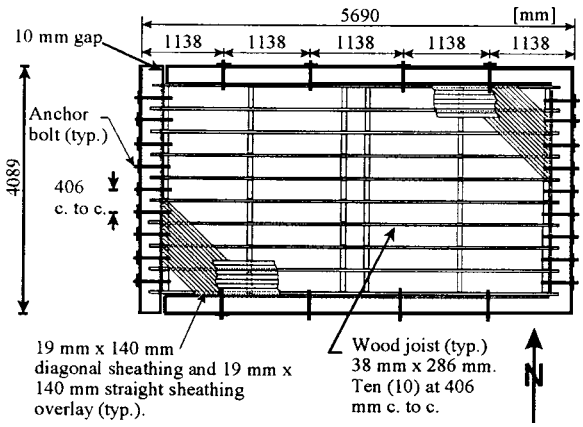

Fig. 3. Wood sheathed diaphragm framing details

two corners of the building were built discontinuous, with vertical gaps left between the shear wall and its perpendicular walls to permit comparison between the plane models considered by many engineers and the actual behavior of building corners.

The specimen has a flexible diaphragm constructed with wood joists covered with diagonal boards with a straight board overlay. The diagonal and straight sheathings consisted of 19 mm $\times$ 140 mm boards, joined with three nails at ends of each board and two nails at all other supports. The diaphragm was anchored to the walls with through-wall bolts in accordance with the special procedure of the UCBC (ICBO 1997). The unreinforced brick masonry specimen was secured to a strong floor by four high strength bolts affixed at each corner of a reinforced concrete foundation. An MTS hydraulic actuator was connected to the specimen's south wall at center span, and at the wood diaphragm level. The actuator was supported by a rigid steel reaction frame as shown in Fig. 4.

Testing Sequence

The pseudodynamic method was used for the majority of the tests conducted on the specimen. The selected input motion is a synthetic ground motion for La Malbaie, Canada (Atkinson and Beresnev 1998), with a peak ground acceleration (PGA) of 0.453*g*. A first series of pseudodynamic tests was conducted on the unreinforced brick masonry specimen. Building design, material properties, construction, instrumentation, and the test results have been discussed elsewhere (Paquette and Bruneau 2003).

In the first series of pseudodynamic tests, the specimen was subjected to the same La Malbaie synthetic time history, scaled to progressively increasing intensity. The unreinforced masonry

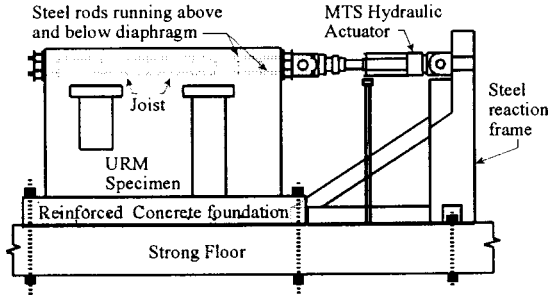

Fig. 4. Test setup

building was tested with La Malbaie $\times$ 0.25, 0.5, 1.0, and 1.5. Finally, the specimen was subjected to La Malbaie $\times$ 2, during which a stable combined rocking and sliding mechanisms formed and large deformations developed without significant strength degradation. The results from these tests for the shear walls were compared with expected performance predicted by different codified equations, notably those from the FEMA 273 (FEMA 1997) and 306 (FEMA 1999) documents (Paquette and Bruneau 2003).

After the first series of tests, the specimen was found to be relatively resilient to earthquake excitation, even though the walls were extensively cracked and the lateral displacements were rather large, corresponding to lateral drift of approximately 1% at La Malbaie $\times$ 2 (PGA approximately 0.9*g*). However, the diaphragm remained essentially elastic throughout. To investigate the effectiveness of repair procedure in increasing the wall lateral load resistance, it was decided to reinforce the shear walls with fiberglass materials. An additional objective of this study was to explore the effect of increased lateral forces developed in the repaired walls to diaphragm response, possibly leading to inelastic deformations.

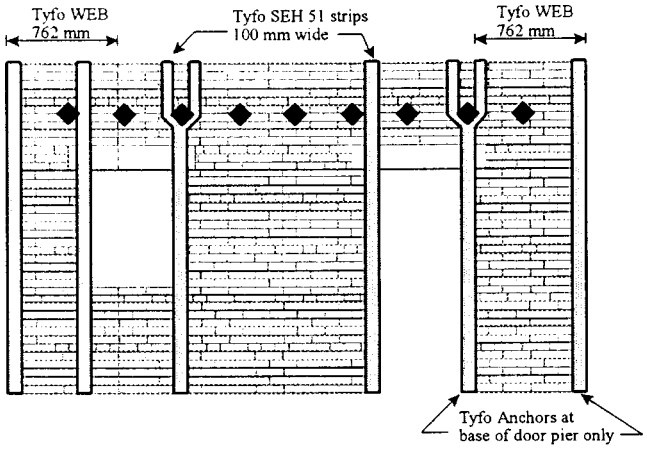

Fig. 5. West wall elevation of unreinforced masonry specimen repaired with Tyfo SEH 51 and WEB (the east wall is simply mirror image)

Repaired Unreinforced Masonry Specimen

Repair Scheme

The repair strategy in this study consisted of strengthening previously damaged URM shear walls with vertical fiber-reinforced composite (FRC) fabric strips externally bonded to the wall surface. The use of FRCs for a variety of industrial applications, mainly related to the rehabilitation or retrofit of existing structures, has rapidly increased in recent years (Ehsani and Saadatmanesh 1997). The main reasons for using composites are their superior strength-to-weight ratios and durability in corrosive environments as compared with the conventional materials and rehabilitation technologies, largely based on the use of cement-based overlays reinforced with steel bars. Previous studies of FRC fabric strips used in masonry rehabilitation focused on enhancing the out-of-plane wall resistance (Reinhorn and Madan 1995a; Ehsani et al. 1999) and in-plane resistance of masonry shear walls failing in diagonal tension failure mode (Madan 1995b). Recent reports and guidelines (NIST 1997, FEMA 1999b) refer to the use of FRC overlays as a viable seismic retrofit technique for enhancing both the in-plane and out-of-plane resistance of URM walls. However, the previous studies have not explored the use of FRCs in retrofitting the masonry walls demonstrating pier rocking behavior.

Fiber Reinforced Composite Fiberglass Fabrics: Installation and Material Properties

E-glass FRC (fiberglass) fabric, manufactured by Hexcel Fyfe Co. of Del Mar, Calif. under the name of Tyfo Fibrewrap system, was used in this study (Tyfo 1997). Two different Tyfo products were used: SEH 51 fabrics bonded with Tyfo S epoxy resin for the vertical tension strips and Tyfo WEB fabric overlay bonded with Tyfo HI-CLEAR adhesive at the wall corners. Two SEH 51 vertical strips (100 mm wide $\times$ 1.3 mm thick) were applied at the ends of each pier (one strip bonded to exterior and interior wall face each), as shown in Fig. 5. Epoxy resin was spread on the clean surface of the brick and the fabric was laid on top of the epoxy. The strips were extended to the top of the parapet, and wrapped along the concrete foundation horizontal base and vertical edge at the bottom of the walls to ensure sufficient anchorage length. Tyfo anchors were used only at the base of the door pier to enhance anchorage at that location because the rocking crack was expected at or near the concrete foundation at that location. In addition, the wall corners were wrapped with WEB fabric overlay (0.4 mm thickness) to increase their shear resistance and to maintain the wall integrity by preventing spalled portions of the wall from falling off and posing a safety hazard.

Based on the information provided by the manufacturer, Tyfo SEH 51 uniaxial tension strips are characterized with ultimate tensile strength of 552 MPa (0° direction) and ultimate elongation of 2%, whereas the modulus of elasticity is equal to 27,579 MPa. The Tyfo WEB fabric is characterized with the bidirectional fiber distribution, resulting in equal ultimate tensile strength of 207 MPa in the 0 and 90° directions, ultimate elongation of 1.5%, and a modulus of elasticity of 13,790 MPa.

Design Procedure

The Tyfo strips were installed at the ends of the piers as it was predicted that they will be the most effective in prolonging the rocking behavior if installed at those locations. Also, the selected locations were subjected to the largest deformations/strains caused by the rocking motion. The repair design was developed based on a simple analytical model assuming masonry–fiberglass fabric strain compatibility along the horizontal pier section. The fiberglass fabric strip was modeled as a uniaxial tension reinforcement using a linear elastic stress-strain relation for the Tyfo SEH51 fiberglass fabric, whereas the rectangular stress block was used for masonry at ultimate per the Canadian Masonry Code (CSA 1994). The tensile force developed in the fiberglass strip and the compressive force developed in masonry were determined from the equation of equilibrium, assuming that the maximum compressive strain in masonry has been reached and that the elongation in fiberglass strip is at 75% of its ultimate value. The corresponding lateral "rocking" force developed in the pier repaired with the fiberglass strips at the ends was determined from the free-body equilibrium of a pier demonstrating rocking behavior, as an extension of the "rocking pier" model proposed by ABK (1984), NRC (1992), and FEMA (1997). The effect of fiberglass strip subjected to compression was neglected. As the objective of the repair was to prolong the desirable rocking behavior, the key

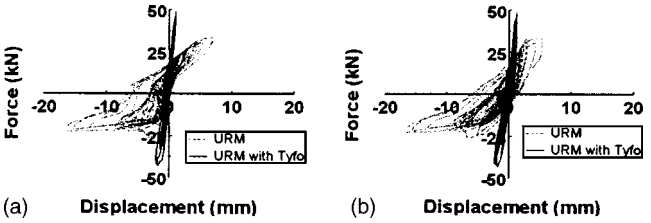

Fig. 6. Hysteretic response of unreinforced masonry during La Malbaie×2.0 before and after Tyfo repair: (a) west wall and (b) east wall

design criterion was to ensure that the rocking lateral force at arbitrarily selected extreme FRC strip strain was less than the corresponding force developed as a result of force-controlled failure (diagonal tension).

Experimental Results of Repaired Specimen

An initial pseudodynamic simulated free vibration test allowed to determine that the period of vibration and the damping ratio of the repaired specimen were 0.12 s and 14.4%, respectively. The repaired specimen was subjected to the same sequence of input motions as used in the testing of the original specimen in order to enable the comparison of response for the two.

Wall Response

During La Malbaie ×0.5 and ×1.0 pseudodynamic tests, the displacements of both east and west shear walls were considerably reduced while maintaining the same level of force as recorded for the original specimen. With the increasing ground motion, during La Malbaie ×1.5 and ×2.0, the wall response was characterized with larger forces and reduced lateral displacements as compared to the original specimen. Hysteretic force–displacement curves for the repaired and original specimen during La Malbaie ×2.0 run are shown in Figs. 6(a and b). It can be observed that the lateral forces in the east and west wall were increased by approximately 48% as compared with the original specimen, whereas the corresponding displacements were considerably reduced. As a result of the increased stiffness of the repaired piers, the rocking motion was significantly reduced, as shown in Fig. 7. The time histories of the diaphragm center-span displacement for the repaired and original specimen for La Malbaie ×2.0 are shown in

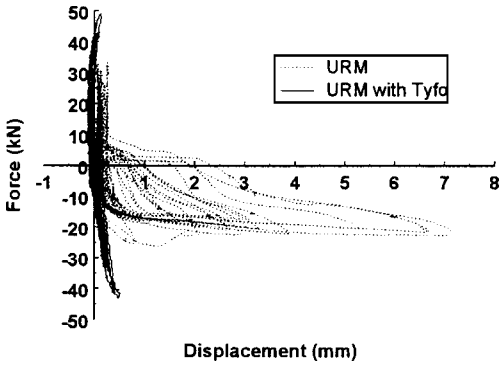

Fig. 7. Door pier rocking response before and after Tyfo repair for La Malbaie×2.0

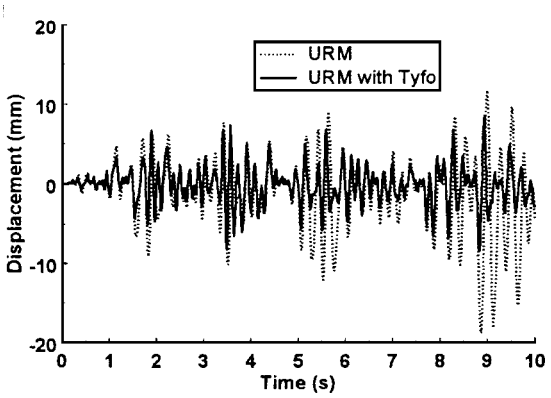

Fig. 8. Comparison of diaphragm center-span response before and after Tyfo repair for La Malbaie×2.0

Fig. 8. Throughout the tests, some noise was heard indicating partial debonding of the Tyfo WEB overlay at the wall corners. The specimen was then subjected to La Malbaie ×3.0 test run, resulting in the development of new cracks in the walls, localized debonding of Tyfo strips, and more noise in the wall corner area repaired with the Tyfo WEB overlay. Due to some unexplained equipment malfunction, the data from that latter test were not fully recovered; therefore, La Malbaie ×3.0 was run a second time. In this second test, some strips as well as the Tyfo WEB overlay at the corner, developed a shearing tear due to the increasing sliding behavior of the central piers in both shear walls. Additional cracks were formed near the concrete foundation below the central pier on the west wall. As the level of excitation was increased, some strips started to debond, yet still providing enough deformation capacity to allow rocking as shown in Fig. 9 (note a visible 10 mm wide crack opening). However, for the central pier demonstrating a bed-joint sliding behavior, the Tyfo strips were mainly subjected to shear stresses and ultimately failed in shear by tearing, as shown in Fig. 10(a). Some tearing was also observed in the Tyfo WEB overlay at the corners due to out-of-plane tensile cracks, as shown in Fig. 10(b). Finally, the specimen was subjected to La Malbaie ×4.0. Additional debonding and tearing of the Tyfo material (strips and WEB) were observed and more extensive cracking developed in the walls, as shown in Figs. 11(a and b).

Due to the limited number of instruments available, only the west shear wall of the specimen was closely instrumented during

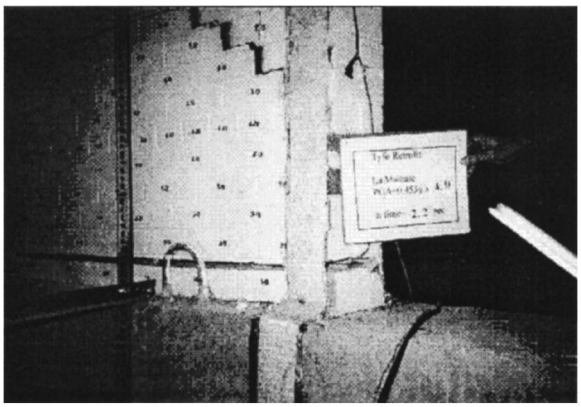

Fig. 9. Pier rocking at base of central pier with Tyfo repair during La Malbaie×4.0

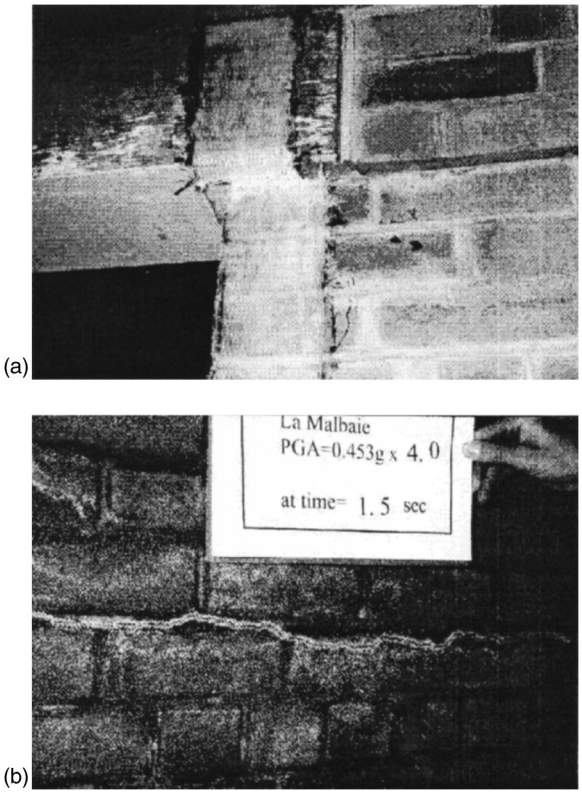

Fig. 10. (a) Tyfo strip failed in shear and (b) tears in Tyfo WEB due to out-of-plane tensile cracks

the early test runs. The clip gages monitoring the cracks on the west wall were then installed on the east wall, and the displacement transducers measuring the in-plane deformation of the diaphragm were moved on the other half. The unreinforced masonry building was then retested with La Malbaie $\times 3.0$ and $\times 4.0$. The Tyfo strips and WEB wall corner overlay completely debonded at some locations and some strips were torn apart. The repeated rocking and sliding behavior of the piers induced tears and debonding, limiting the wall capacity to approximately 66 kN, resulting in increased lateral displacements, as observed in Fig. 12. Note that the hysteretic curves obtained for the west and east walls are fairly similar.

Diaphragm Response

Strengthening the shear walls with Tyfo materials did increase the force on the diaphragm, as shown in Fig. 13, comparing diaphragm response with shear walls as-is and repaired with Tyfo for La Malbaie $\times 2.0$. At La Malbaie $\times 4.0$ for the repaired specimen,

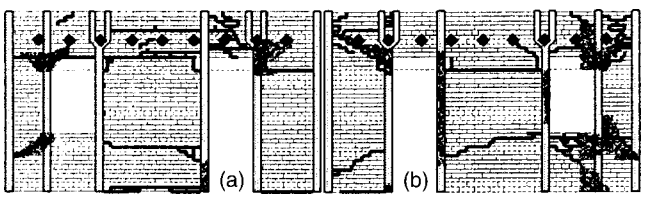

Fig. 11. Crack pattern on repaired shear wall after La Malbaie $\times 4.0$: (a) west wall and (b) east wall (shaded area indicates Tyfo material debonded)

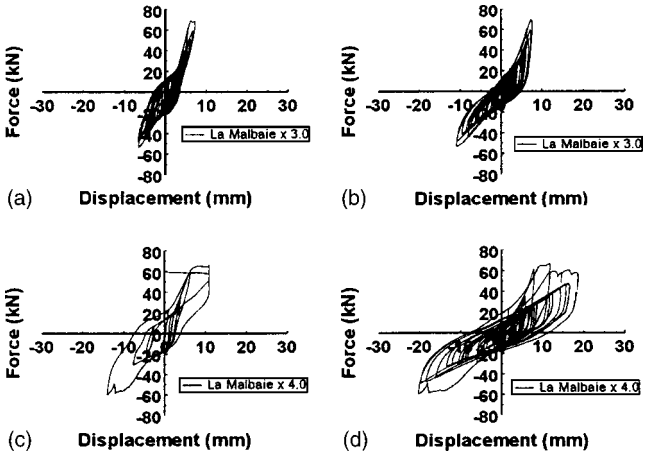

Fig. 12. Hysteretic response of unreinforced masonry with Tyfo during: La Malbaie $\times 3.0$: (a) west wall, (b) east wall; and La Malbaie $\times 4.0$: (c) west wall and (d) east wall

some nonlinear diaphragm behavior initiated, as seen in Fig. 14. However, due to the state of damage on the shear walls, and for safety reasons, it was decided at this point to proceed further using conventional quasistatic cyclic tests, by simply increasing the center-span displacement instead of continually increasing the input motion in pseudodynamic tests.

Cyclic Quasistatic Testing

The center-span displacement of the specimen was increased by pushing with the actuator with a predetermined set of displacements i.e., 1.0, 1.5, 2.5, and 3.0% drift until a large proportion of the Tyfo materials (strips and WEB) were almost completely debonded from the shear wall surface. The hysteretic curves and the final crack pattern are shown in Figs. 15 and 16, respectively. However, because of horizontal cracks in both shear walls at the top of each pier, and because most of the Tyfo material had debonded and became ineffective in strengthening these shear walls, the diaphragm simply slid back and forth over the top of each pier like a rigid body when pushed with the actuator. Hence, the diaphragm did not experience any additional nonlinear inelastic behavior. After the test, examination showed that the diaphragm remained relatively intact. Damage was limited to some popped out nails at each ends of the diaphragm.

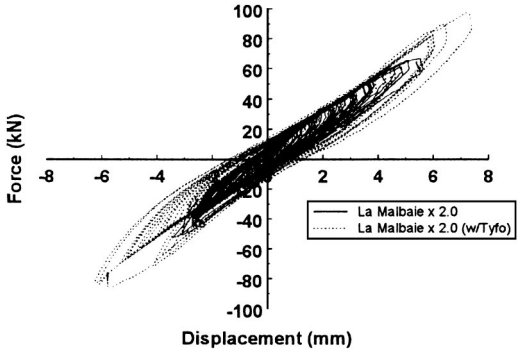

Fig. 13. Comparison of hysteretic response of wood diaphragm with shear walls as-is and repaired with Tyfo, during La Malbaie $\times 2.0$

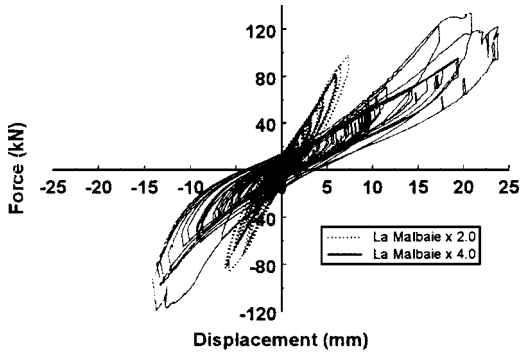

Fig. 14. Comparison of diaphragm center-span hysteretic response with shear wall repaired with Tyfo material during La Malbaie $\times 2.0$ and $\times 4.0$

Evaluation of Wood Diaphragm Response

Models and Theoretical Values

The dynamic response of the wood diaphragm was also investigated. It is addressed specifically in various documents such as the UCBC (ICBO 1997), the *NEHRP Handbook for Seismic Evaluation of Existing Buildings* (FEMA 1992), the Canadian Guidelines for Seismic Evaluation of Existing Buildings (CGSEEB) (NRC 1992), and the Prestandard and Commentary for the Seismic Rehabilitation of Buildings (FEMA 2000). In the CGSEEB, FEMA 178, and the UCBC, the dynamic response is essentially assessed by calculating a normalized demand–capacity ratio (DCR). Given that the CGSEEB, FEMA 178, and UCBC requirements are essentially similar, for the sake of brevity, equations and calculations are shown for the CGSEEB only. Thus, the DCR is given by

$$\text{DCR} = \frac{2.5v'W_d}{\sum v_u D} \tag{1}$$

where v_u, W_d, D, and v' = respectively, unit shear, total load tributary to the diaphragm, width of the diaphragm, and effective velocity ratio defined by

$$v' = \frac{v\text{IF}}{1.3} \leqslant 0.4I \tag{2}$$

where v = zonal velocity ratio; I = importance factor; and F = foundation factor typically found in the National Building Code of Canada (NRC 1995). For the special evaluation methodology to be applicable, any given point defined by the DCR and the span L must fall within the boundaries of the graph in Fig. 17 (NRC 1992). This figure has been developed to control the severity of

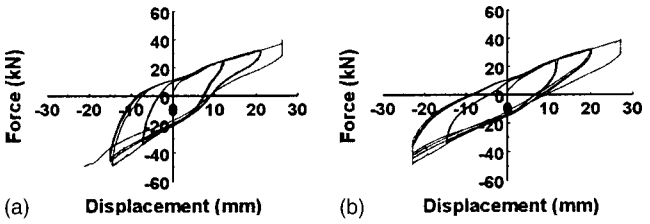

Fig. 15. Hysteretic response during cyclic test: (a) west wall and (b) east wall

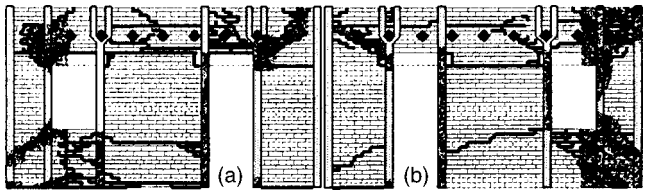

Fig. 16. Crack pattern on shear wall repaired with Tyfo after cyclic test: (a) west wall and (b) east wall (shaded area indicates Tyfo material debonded)

the diaphragm displacements and velocities at mid-span. It also ensures that the horizontal deflection of the diaphragm does not produce instability of the out-of-plane walls by providing limits on slenderness ratios derived from dynamic stability concepts. The figure is divided into three regions, namely: Region 1 where h/t ratios for buildings with cross walls may be used if qualifying cross walls are present in all stories; Region 2 where h/t ratios for buildings with cross walls may be used whether or not qualifying cross walls are present; and Region 3 where h/t ratios for other buildings shall be used whether or not qualifying cross walls are present.

Using $v' = 0.4$, $W_d = 114.5$ kN, $v_u = 29.8$ kN/m, and $D = 3.66$ m for the tested specimen, the DCR is 1.05, and given the diaphragm span of 5.28 m, it is confirmed that the point (1.05, 5.28) falls in Region 3 of Fig. 17.

FEMA 356 defines the capacity of a diaphragm by its yield shear capacity. Typical values for chorded and unchorded (i.e., presence or not of perimeter chord or flange members) wood

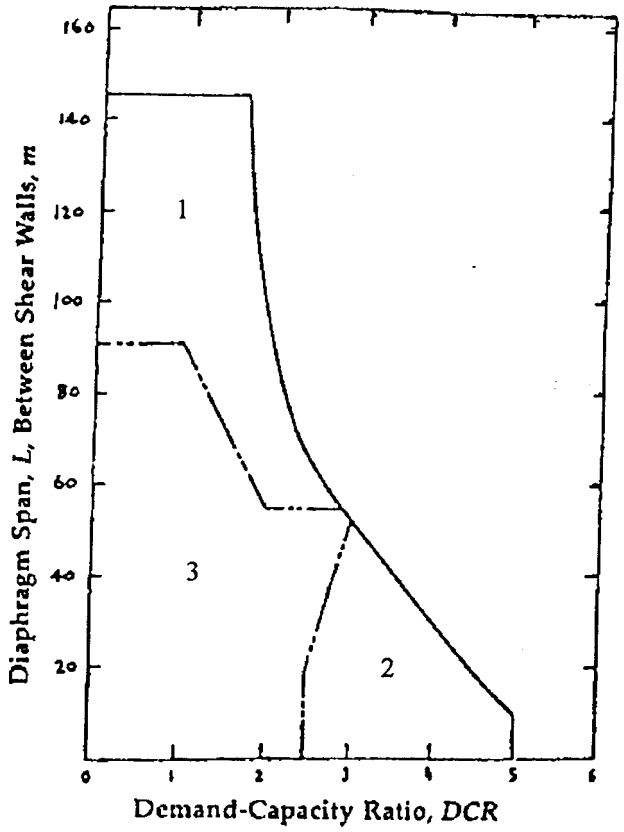

Fig. 17. Figure of acceptable diaphragm span versus demand-capacity ratio (NRC 1992)

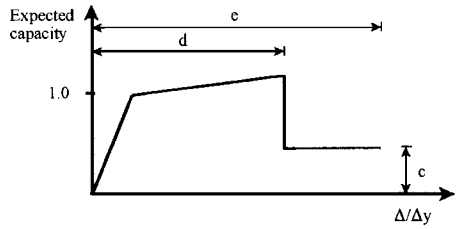

Fig. 18. Federal Emergency Management Agency 356 generalized force–deformation relation for wood diaphragm

diaphragm having diagonal sheathing with straight sheathing overlay are 13.13 kN/m (900 lb/ft) and 9.12 kN/m (625 lb/ft), respectively (FEMA 2000).

The elastic maximum deflection of a wood diaphragm is given by

$$\Delta = \frac{v_y L}{2G_d} \tag{3}$$

where v = shear at yield in the direction under consideration; L = diaphragm's span; and G_d = diaphragm shear stiffness taken as 3,152 kN/m (18,000 lb/in) and 1,576 kN/m (9,000 lb/in) for chorded and unchorded diagonal sheathing with straight sheathing, respectively (FEMA 2000).

The nonlinear inelastic deformation of the diaphragm is determined by a generalized force–deformation relation defined by parameters d, e, and c, as shown in Fig. 18, where d is the maximum deflection at the point of first loss of strength taken as 1.5 times the yield strength, and e is the maximum deflection at a reduced strength c. These values are given in Table 1, for a diaphragm with straight sheathing over diagonal sheathing.

Alternatively, the ABK methodology (ABK 1982) expresses force–deformation envelopes for different type of wood diaphragms by a second-order curve defined by

$$F(e) = \frac{F_u e}{\frac{F_u}{k_i} + e} \tag{4}$$

where $F(e)$ = force at the diaphragm's end; e = mid-span deformation; k_i = initial stiffness; and F_u = ultimate force (asymptote). The ultimate force F_u is given by the unit shear strength of the diaphragm v_u multiplied by its width D. Properties of typical diaphragms are given in Table 2. Scaling of the initial stiffness given in Table 2 for diaphragms with different sizes can be performed using the following relationship (ABK 1982):

$$k_2 = \frac{d_2}{d_1}\frac{l_1}{l_2}k_1 \tag{5}$$

where k_1 = initial stiffness of a diaphragm of size $l_1 \times d_1$; and k_2 = initial stiffness of a diaphragm of size $l_2 \times d_2$. For a wood diaphragm having diagonal sheathing with straight sheathing overlay, the initial stiffness from Table 2 is 10.7 kN/mm for a 6.1 m × 6.1 m diaphragm. Using Eq. (5), the initial stiffness for a 3.66 m × 5.28 m diaphragm is

$$k_2 = \frac{(3.66)(6.1)}{(6.1)(5.28)}10.7 = 7.42 \text{ kN/mm} \tag{6}$$

The unit shear strength, 29.8 kN/m (from Table 2) multiplied by the diaphragm's width, 3.66 m, gives the ultimate force F_u = 109.1 kN for the diaphragm's dimensions considered here.

Table 1. Federal Emergency Management Agency, 356 Modeling Parameters for the Generalized Force–Deformation Relation for Wood Diaphragm with Straight Sheathing over Diagonal Sheathing

Diaphragm type	Aspect ratio L/b	d	e	c
Chorded	≤2.0	3.0	4.0	0.2
Unchorded	≤2.0	2.5	3.5	0.3

Table 2. Properties of Typical Diaphragms (6.1 m × 6.1 m) Based on Agbabian, Barnes, and Kariotis

Diaphragm type	Unit shear (kN/m)	Initial stiffness (kN/mm)
19 mm × 140 mm straight sheathing	4.8	2.33
19 mm × 140 mm diagonal sheathing	11.6	8.27
19 mm × 140 mm diagonal sheathing + 19 mm × 140 mm straight sheathing overlay	29.8	10.7
19 mm plywood + 19 plywood overlay	42.1	8.66

Comparison with Experimental Results

Using the data recorded by the three temposonics located across the span of the diaphragm as well as the LVDTs on each shear wall, the lateral force–deformation relationship of the diaphragm was investigated. The hysteretic response of the wood diaphragm during La Malbaie × 2.0 is shown in Fig. 19, and is essentially linearly elastic. The maximum floor deformation (center relative to ends) recorded at mid-span was 5.54 mm under a 66.5 kN force. Using Eq. (3) from FEMA 356, the calculated mid-span deflection is 7.61 mm for chorded diaphragm. For the sake of comparison, FEMA 273 which uses a slightly different equation is also included in Fig. 19.

Using the force–deformation envelope from ABK, Eq. (4), and rearranging the terms, gives

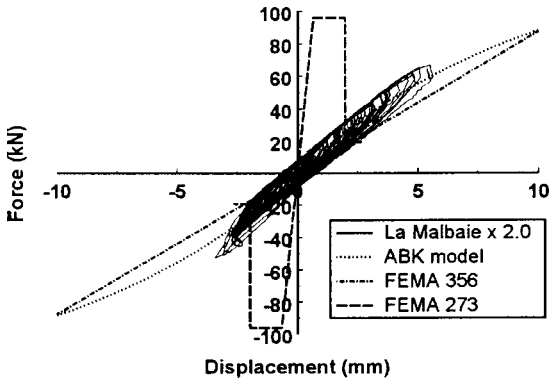

Fig. 19. Comparison of hysteretic response of wood diaphragm during La Malbaie × 2.0 with Federal Emergency Management Agency 356 and 273, and Agbabian, Barnes, and Kariotis force–deformation relations

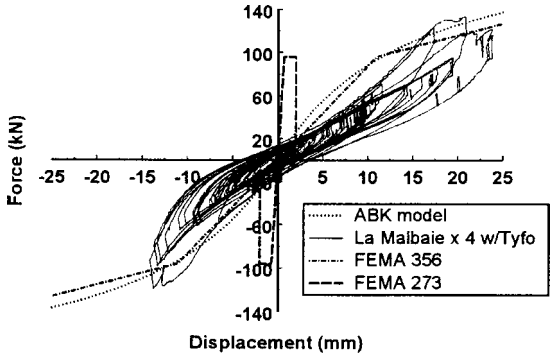

Fig. 20. Hysteretic response of wood diaphragm with shear walls repaired with Tyfo for La Malbaie × 4.0, with Federal Emergency Management Agency 356 and 273, and Agbabian, Barnes, and Kariotis force–deformation relations

$$e = \frac{\frac{F_u}{k_i}F(e)}{F_u - F(e)} \tag{7}$$

Thus, for a force of 33.25 kN (i.e., 66.5/2 kN) at the end of the diaphragm, the calculated deflection, using Eq. (7) is 6.45 mm, which also matches closely the experimentally obtained deflection.

The in-plane lateral load-resisting capacity of the repaired shear walls was increased as compared to the original walls. As a result, larger forces were developed, thus inducing larger relative displacements between the diaphragm and shear walls. As observed in Fig. 20, a maximum mid-span deflection of 23.9 mm was recorded under a load of 115.8 kN for La Malbaie × 4.0. Corresponding deformations under such load using Eq. (7) is 16.6 mm for the ABK model, and 20.0 mm for chorded diaphragm using the force–deformation relation from FEMA 356. Again, both FEMA 356 and ABK give diaphragm deflections relatively close to those obtained experimentally. Experimental results for the diaphragm closely follow the FEMA 356 and ABK models in the linear elastic range, but since the diaphragm did not undergo very large inelastic deformations, it is not known whether it would behave as predicted by both models up to its ultimate. For the sake of comparison FEMA 273, which uses a slightly different equation, is also included in Fig. 20.

Deflected Shape

Even though the diaphragm was restricted by continuous corners on one side, the experimentally obtained in-plane deflected shape of the diaphragm for the original specimen is nearly symmetric and close to that of a pinned-pinned beam model, as shown in Fig. 21. Interestingly, the deflected diaphragm shape for the repaired specimen is no longer symmetrical. In that case, the continuous corners wrapped with Tyfo WEB seem to have restrained the rotation of the diaphragm at that end, compared to the discontinuous corners, where the Tyfo WEB provided limited resistance along the gap, leading to tearing over the height. Although a pinned–pinned model was a good match for the deflected diaphragm shape of the original specimen, a fixed–pinned model more accurately captures the deflected diaphragm shape for the repaired specimen. The parabolic shape observed suggests that flexural deformations dominated over shear deformations for this diaphragm. Given that the relationship proposed by FEMA 273

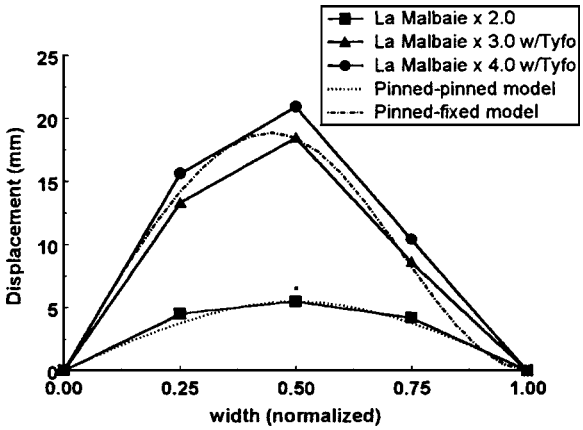

Fig. 21. Deflected shape of wood diaphragm during La Malbaie × 2.0, 3.0, 4.0, and matching pinned–pinned, pinned–fixed beam models

was not comparing well with the observed results, and looking at the parabolic shape, different flexural beam models were investigated even though the deflections observed experimentally closely matched those predicted using the FEMA 356 and ABK models. Assuming that the deflection can be computed using a fixed–pinned beam model, using the modulus of elasticity of Spruce (i.e., $E = 9,500$ MPa), different models for the moment of inertia were investigated to match the experimental and analytical results.

Model 1

A first approach calculates the flexural deflection of the floor, as a composite system, but neglecting the sheathing shear deformation as shown in Fig. 22. As a conservative first approach, only the two outer joists are considered in calculating the floor inertia. The corresponding moment of inertia of this section is 7.129×10^{10} mm^4. Using this value in a fixed-pinned beam model to calculate the deflection for La Malbaie × 4.0 gives 0.264 mm, significantly less than the 23.9 mm observed experimentally. This suggests that a flexural model that assumes full in-plane compositeness of the wood floor is not appropriate.

Model 2

An alternative approach assumes that the flexural stiffness of the diaphragm is given by the sum of the weak-axis flexural stiffness of the wood joists, with one of the outer joists treated as behaving in a composite manner with the adjacent brick wall as shown in Fig. 23. Indeed, because the joist at the outer edge of the diaphragm is continuously tied to the masonry wall by anchors, a section of the brick wall is engaged and can contribute to the stiffness of the diaphragm. Equivalent stiffness of that joist is

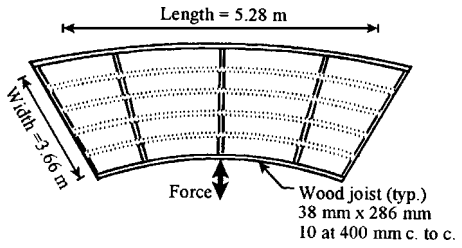

Fig. 22. Wood diaphragm deflected shape (model 1)

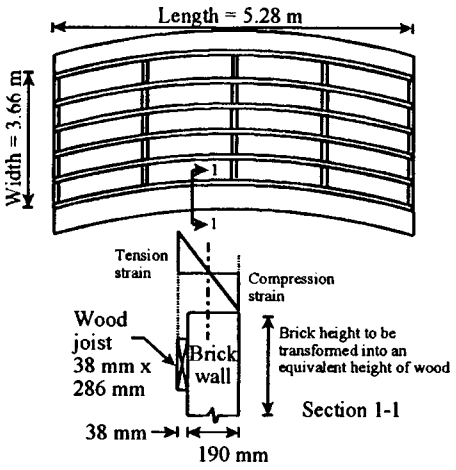

Fig. 23. Wood diaphragm deflected shape (model 2)

therefore calculated using the modular ratio, transforming the effective brick wall into an equivalent height of wood. Note that, by analogy, this wood–masonry composite joist is conceptually similar in behavior to that of a reinforced concrete beam, with the wood joist acting as the reinforcing bar in tension and the brick wall as the concrete in compression. The portion of brick wall participating into the diaphragm stiffness is assessed empirically. To match the deflection obtained experimentally, a 1,500 mm height of brick is required to contribute. This value would correspond to 286 mm over the joist depth, 258 mm for the parapet above, and an additional 956 mm of brick wall below the joist, which seems to be reasonable. Then, the inertia of the wood–masonry composite joist is 1.0483×10^9 mm^4, and the inertia of the remaining nine joists is $9\times(1.308\times10^6)=1.177\times10^7$ mm^4. Thus, the total inertia is 1.060×10^9 mm^4. Using a fixed–pinned beam model, it gives a mid-span deflection of 18.5 mm, matching the deflection obtained experimentally for La Malbaie $\times$ 3.0, 18.49 mm.

Thus, even though the diaphragm did not have a long span (aspect ratio = 1.44), the lateral deflection of the wood diaphragm was mostly due to flexural rather than shear deformations. The fact that the joists were laid parallel to the long diaphragm direction as opposed to spanning the short direction, as commonly encountered, may have contributed to the observed flexural deformation, but the concept underlying Model 2 appears applicable to any aspect ratio.

In-Plane Deformation

Two Celesco displacement transducers were used to measure the in-plane deformation of the diaphragm as reported in Paquette and Bruneau (2003). The resulting hysteretic response is shown in Figs. 24(a and b) for La Malbaie $\times$ 2.0 without Tyfo and $\times$4.0 with Tyfo repair, respectively. The odd response observed can be explained as follows, and is schematically illustrated in Fig. 25. First, the top layer of straight sheathing is assumed to bend back and forth following the imposed displacement in the north–south direction without contributing much to the diaphragm strength or stiffness. Therefore, the displacement transducers are assumed to measure displacements as affected by the diagonal sheathing. As such, the transducer parallel to the bottom layer of diagonal sheathing (labelled "celesco north" in Fig. 25) measures planks elongation in tension or compression, which explains the relatively high rigidity observed by that instrument, while the perpendicular displacement transducer (labelled "celesco south") measures the lateral separation of these planks, which explains the lesser rigidity and larger displacement observed in that direction. The same behavior was observed when the displacement transducers were installed on the other half of the diaphragm.

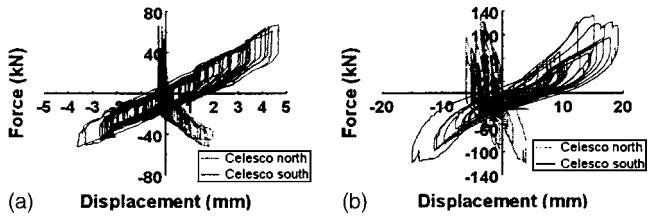

Fig. 24. Hysteretic response of in-plane wood diaphragm deformation during: (a) La Malbaie $\times$ 2.0 without Tyfo and (b) La Malbaie $\times$ 4.0 with Tyfo

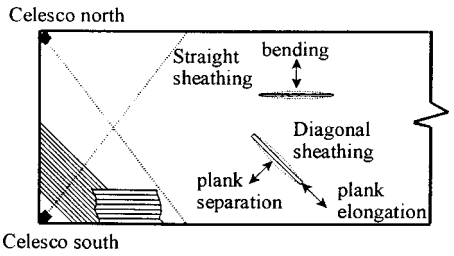

Fig. 25. Schematic illustration of in-plane diaphragm deformation

Conclusions

A full-scale one-story unreinforced brick masonry specimen having a flexible wood diaphragm was tested pseudodynamically. The specimen was repaired using Tyfo fiberglass strips, which increased the lateral strength of the shear wall while significantly reducing the displacements. While subjected to higher force, the diaphragm exhibited some nonlinear inelastic behavior. Although not tested to its ultimate capacity, it was shown to deflect primarily due to flexural deformation as opposed to shear deformation as commonly assumed. The diaphragm deflections observed experimentally closely matched those predicted using the FEMA 356 and ABK models.

Acknowledgments

The writers acknowledge the financial support provided by the Natural Science and Engineering Research Council of Canada (NSERC), Brampton Brick, Fitzgerald Building Supplies (1996) Limited, Ottawa Region Masonry Contractors Association, International Union of Brick Layers and Allied Craftsmen (Industrial Promotion Fund), Canadian Portland Cement Association, George and Asmussen Limited, R.J. Waston Inc., and Fyfe Co. L.L.C. However, conclusions and opinions expressed in this paper are those of the writers alone.

References

Agbabian & Associates, S.B. Barnes & Associates, and Kariotis & Associates, (ABK) A Joint Venture. (1982). "Methodology for mitigation of seismic hazards in existing unreinforced masonry buildings: Interpretation of diaphragm tests." *Rep. No. ABK-TR-05 (draft)*, El Segundo, Calif.

Agbabian & Associates, S.B. Barnes & Associates, and Kariotis & Associates, (ABK) A Joint Venture. (1984). "Methodology for mitigation of seismic hazards in existing unreinforced masonry buildings: The methodology." *Rep. No. ABK-TR-08*, El Segundo, Calif.

Atkinson, G., and Beresnev, I. (1998). "Compatible ground-motion time histories for new national seismic hazard maps." *Can. J. Civ. Eng.*, 25, 305–318.

Bruneau, M. (1994). "Seismic evaluation of unreinforced masonry buildings - a state-of-the-art report." *Can. J. Civ. Eng.*, 21(3), 512–539.

Canadian Standards Association, (CSA). (1994). "Masonry design for buildings." *CSA Standard S304. 1-94*, Rexdale, Ontario, Canada.

Costley, A.C., and Abrams, D.P. (1995). "Dynamic response of unreinforced masonry buildings with flexible diaphragms." *Rep. No. UILU-ENG-95-2009*, Dept. of Civil Engineering, Univ. of Illinois at Urbana-Champaign, Urbana, Ill.

Ehsani, M.R., and Saadatmanesh, H. (1997). "Fiber composites: An economical alternative for retrofitting earthquake-damaged precast-concrete walls." *Earthquake Spectra* 13(2), 225–241.

Ehsani, M.R., Saadatmanesh, H., and Velazquez-Dimas, J.I. (1999). "Behavior of retrofitted URM walls under simulated earthquake loading." *J. Compos. Constr.*, 3(3), 134–142.

Epperson, G.S., and Abrams, D.P. (1990). "Evaluating lateral strength of existing unreinforced brick piers in the laboratory." *Proc., 5th North American Masonry Conf.*, Vol. 2, Urbana-Champaign, Ill., 735–746.

Federal Emergency Management Agency (FEMA) (1992). *NEHRP handbook for the seismic evaluation of existing buildings*, *FEMA 178*, Building Seismic Safety Council, Washington, D.C.

Federal Emergency Management Agency (FEMA) (1997). "NEHRP guidelines for the seismic rehabilitation of buildings." *FEMA 273* Building Seismic Safety Council, Washington, D.C.

Federal Emergency Management Agency (FEMA). (1999a). "Evaluation of earthquake damaged concrete and masonry wall buildings, basic procedures manual." *FEMA 306*, The Patnership for Response and Recovery, Washington, D.C.

Federal Emergency Management Agency (FEMA). (1999b). "Repair of earthquake damaged concrete and masonry wall buildings." *FEMA 308*, Washington, D.C.

Federal Emergency Management Agency (FEMA). (2000). "Prestandard and commentary for the seismic rehabilitation of buildings." *FEMA 356*, Washington, D.C.

International Conference of Building Officials (ICBO). (1997). "Uniform code for building conservation." Whittier, Calif.

National Institute of Standards and Technology (NIST). (1997). "Development of procedures to enhance the performance of rehabilitated URM buildings." *Rep. No. NIST GCR 97-724-1*, Building and Fire Research Laboratory, Gaithersburg, Md.

National Research Council (NRC). (1992). "Guidelines for seismic evaluation of existing buildings." Institute for Research in Construction, Ottawa.

National Research Council of Canada (NRC). (1995). "National building code of Canada." Ottawa.

Paquette, J., and Bruneau, M. (2003). "Pseudo-dynamic testing of unreinforced masonry building with flexible diaphragm." *J. Struct. Eng.* 129(6), 708–716.

Prawel, S.P., and Lee, H.H. (1990). "The performance of upgraded brick masonry piers subjected to out-of-plane motion." *Proc., 4th National Conf. on Earthquake Engineering*, Vol. 3, Palm Springs, Calif., 273–281.

Reinhorn, A.M., and Madan, A. (1995a). "Evaluation of TYFO-W fiber wrap system for out of plane strengthening of masonry walls." *Preliminary Test Rep. No. AMR95-0001*, Dept. of Civil Engineering, State Univ. of New York, Buffalo, N.Y.

Reinhorn, A.M., and Madan, A. (1995b). "Evaluation of TYFO-W Fiber Wrap System for In Plane Strengthening of Masonry Walls." *Test Rep. No. AMR95-0002*, Dept. of Civil Engineering, State Univ. of New York, Buffalo, N.Y.

Tyfo (1997). "Tyfo systems for unreinforced masonry (URM) and reinforced concrete/masonry wall strengthening." Fyfe Co. L.L.C., San Diego.